Self-Validated Time-Domain Analysis of Linear Systems with Bounded Uncertain Parameters

Self-Validated Time-Domain Analysis of Linear Systems with Bounded Uncertain Parameters

Riccardo Trinchero, *Member, IEEE,* Paolo Manfredi, *Member, IEEE,* Igor S. Stievano, *Senior Member, IEEE.*

***Abstract*—This paper presents a novel approach to predict the bounds of the time-domain response of a linear system subject to multiple bounded uncertain input parameters. The method leverages the framework of Taylor models in conjunction with the numerical inversion of Laplace transform (NILT). Different formulations of the NILT are reviewed, and their advantages and limitations are discussed. An implementation relying on an inverse fast Fourier transform (IFFT) turns out to be the most efficient and accurate alternative. The feasibility of the technique is validated based on several diverse application examples, namely a control loop, a lossy transmission-line network and an active low-pass filter.**

***Index Terms*—Circuit simulation, numerical inversion of Laplace transform, Taylor models, uncertainty.**

I. Introduction

The increasing variability in the manufacture of electronic components has recently prompted a wide interest in accurate techniques for the quantification of uncertainties that, if not properly accounted for, may severely affect design costs and time to market. Uncertainty quantification techniques are indeed of paramount importance in modern designs to flag potential problems prior to mass fabrication and avoid expensive redesign. In this framework, it is often useful to estimate the strict upper and lower bounds of the system performance, for example to take into account approximations or truncation of input data, or whenever the actual distribution of such data is unknown.

Interval methods are *self-validated* algebraic techniques, meaning that they provide a conservative enclosure of the solution of a system subject to bounded uncertain input parameters. Interval analysis and affine arithmetic are two interval techniques that were both applied to the worst-case analysis of electrical circuits (see [1] and [2], respectively). However, they suffer from some limitations arising from the lack of, or rough parametrization with respect to the uncertain input parameters, which leads to potentially large overestimation and little insight into their relationship with the outputs of interest [3].

The Taylor arithmetic, or Taylor model (TM), is an alternative approach that combines the robustness of the interval analysis and the strength of a higher-order parametric representation [4]–[5]. Each TM variable consists of a multivariate Taylor polynomial, providing an accurate parametric representation with respect to the uncertain input parameters, which is complemented by an interval remainder accounting for approximation and round-off errors arising in the calculation of the system solution. Hence, the upper and lower bounds of a TM variable are readily determined from those of its polynomial part. The methodology was recently adapted for the first-time application to the frequency-domain analysis of linear circuits [6], and it was later improved and integrated into a freely available general purpose tool [7], [8].

The applicability of this approach to time-domain analysis was however still questionable. In general, some applications of TMs to the solution of ordinary differential equation (ODE) systems were discussed in the literature [9]–[11]. However, most of the applications appear to be limited to very small-size problems in terms of number of unknowns. Furthermore, some issues were reported concerning the blowup of the enclosure (remainder) as integration progresses over time [11].

The present paper proposes an alternative approach that overcomes the aforementioned limitations, by leveraging the state-of-the-art TMsim tool [7] in conjunction with the numerical inversion of Laplace transform (NILT) [12]–[15]. Indeed, working in the Laplace domain provides several advantages:

- the conservativity of the remainder through the transform is guaranteed by the linearity of the Laplace operator;
- the remainder blowup can be avoided, or considerably reduced, if the solution of every time point is cast as an independent contribution from different complex frequencies;
- issues related to the proper time step choice, which can become critical in time-domain integrations, especially for active and/or highly resonating circuits, are avoided;
- the inclusion of components that are inherently defined in the frequency domain, like control loops or lossy and dispersive transmission lines, becomes straightforward;
- it offers the possibility to simulate larger problems, as the solution relies on the effective and robust algorithm for matrix inversion proposed in [6], rather than on cumbersome time-domain numerical integrations.

Nevertheless, there exist several implementations of the NILT. Three alternative approaches, based on inverse fast Fourier transform (IFFT), Padé approximation, and convolution, are reviewed and compared in this paper. Their advantages and limitations are highlighted, showing that the IFFT-based NILT provides the best accuracy and computational

This work was supported in part by the Research Foundation Flanders (FWO).

R. Trinchero and I. S. Stievano are with the EMC Group, Department of Electronics and Telecommunications, Politecnico di Torino, 10129 Torino, Italy (e-mail: riccardo.trinchero@polito.it; igor.stievano@polito.it).

P. Manfredi is with the Electromagnetics Group, Department of Information Technology, IDLab, Ghent University – imec, 9052 Gent, Belgium (e-mail: paolo.manfredi@ugent.be).

efficiency. The discussion is supported by three application examples.

II. Taylor Model

The standard TM representation of a generic function $f(\mathbf{x})$, with $\mathbf{x}$ in a bounded domain[1] $D \subset \mathbb{R}^d$, is

$$f(\mathbf{x}) = P_f(\mathbf{x}) + I_f, \tag{1}$$

where $P_f(\mathbf{x})$ is a polynomial up to a predefined order n, whereas $I_f = [\underline{I_f}, \overline{I_f}]$ is a two-valued interval remainder. While $P_f(\mathbf{x})$ provides in fact an approximate parametric representation of $f(\mathbf{x})$ over D, the interval remainder is such that

$$P_f(\mathbf{x}) + \underline{I_f} \leq f(\mathbf{x}) \leq P_f(\mathbf{x}) + \overline{I_f} \quad \forall \mathbf{x} \in D, \tag{2}$$

i.e., the true value of $f(\mathbf{x})$ is guaranteed to lie between the upper and lower curves defined by the polynomial $P_f(\mathbf{x})$ and the interval remainder I_f. Based on the above property, it is possible to conclude that the global extrema of $f(\mathbf{x})$ are

$$\min_{\mathbf{x}\in D}\{f(\mathbf{x})\} \geq \min_{\mathbf{x}\in D}\{P_f(\mathbf{x})\} + \underline{I_f} \tag{3a}$$

$$\max_{\mathbf{x}\in D}\{f(\mathbf{x})\} \leq \max_{\mathbf{x}\in D}\{P_f(\mathbf{x})\} + \overline{I_f}. \tag{3b}$$

A conservative estimation of the extrema of the multivariate polynomial, which cannot be determined in closed form, is obtained by using the properties of Bernstein polynomials [6].

The problem then amounts to express the output quantity of interest in the form (1). This is achieved by propagating the TM representation starting from the selected uncertain input parameters and through a suitable redefinition of the operations involved in the calculation of the output [6], [7]. Once (1) is determined, the property (3) is used to conservatively estimate the upper and lower bounds of the uncertain output variable. The TM representation (1) is suitably extended to matrix arithmetic. In particular, the inversion of a matrix TM is effectively carried out leveraging the Sherman-Morrison formula [6].

The outlined TM framework is readily applied to the estimation of the upper and lower bounds of the Laplace-domain response $Y(s;\mathbf{x})$ of a generic linear network with bounded uncertain parameters $\mathbf{x}$.

III. Time-Domain Analysis via TM and NILT

The time-domain response $y(t)$ of a linear system can be obtained from its Laplace-domain response $Y(s)$ via the inverse Laplace transform, which reads

$$y(t) = \mathscr{L}^{-1}\{Y(s)\}(t) = \frac{1}{j2\pi}\int_{\sigma-j\infty}^{\sigma+j\infty} Y(s)e^{st}ds, \tag{4}$$

where $s = \sigma + j\omega$ is the Laplace variable consisting of the dumping term $\sigma > 0$ and the angular frequency ω. Thanks to the linearity of the Laplace operator, the TM of a Laplace-domain response can be directly transformed into the corresponding time-domain TM without introducing issues on the conservativity of its remainder.

In general, however, an exact closed-form solution of the above integral is not available for large scale circuit. Indeed, large networks are solved numerically and their responses are usually available as tabulated data. For this reason, in the last decades different techniques have been proposed for the numerical solution of (4). In particular, three NILT techniques are investigated in the following, with the aim of assessing their advantages and limitations in view of the targeted application to the time-domain self-validated analysis of linear systems.

A. NILT Based on IFFT

The inverse Laplace transform in (4) can be rewritten in terms of the inverse Fourier transform as follows:

$$\begin{aligned} y(t) =& \frac{e^{\sigma t}}{j2\pi}\int_{-\infty}^{+\infty} Y(\sigma + j\omega)e^{j\omega t}d\omega = \\ =& e^{\sigma t}\mathscr{F}^{-1}\{Y(\sigma + j\omega)\}(t) = e^{\sigma t}\tilde{y}(t). \end{aligned} \tag{5}$$

where the signal $\tilde{y}(t) = y(t)e^{-\sigma t}$ is a dumped version of the actual time-domain response $y(t)$.

The above integral can be efficiently computed with the robust and well-known IFFT algorithm, leading to

$$y(t_k) = e^{\sigma t_k}\underbrace{\Delta_f \sum_{n=0}^{+N} \Re e\left\{c_n Y(\sigma + j2\pi n\Delta_f)e^{j2\pi n\Delta_f t_k}\right\}}_{\tilde{y}(t_k)}, \tag{6}$$

where $c_0 = 1$, $c_n = 2\ \forall n > 0$, $\Delta_f = 1/T_w$ is the sampling frequency determined by the desired observation time window T_w, and $t_k = kT_w/N \in [0, T_w]$ is the kth discrete time instant. In order to minimize the time-domain aliasing error introduced by the discrete spectrum of $Y(s)$, a damping factor of $\sigma = \alpha\ln(N)/T_w$ with $\alpha > 1$ is usually considered to ensure that $\tilde{y}(t)$ decays to zero at the end of the observation window $[0, T_w]$ [12], [13].

It should be noted that (6) merely involves a linear combination of samples of Laplace-domain responses evaluated at a *fixed* set of complex frequency points. This calculation can be readily carried out using the available TM operations [7]. The term $e^{\sigma t_k}$ may slightly increase the remainder towards the end of the time window but, as shown by the application examples, this effect is limited by considering $\alpha = 1.5$.

B. NILT Based on Padé Approximation

The discussion starts by introducing in (4) the variable change $z = st$, which leads to the following integral [15]:

$$y(t) = \frac{1}{j2\pi t}\int_{\sigma'-j\infty}^{\sigma'+j\infty} Y\left(\frac{z}{t}\right)e^{z}dz. \tag{7}$$

The Padé approximation of the exponential function reads

$$e^{z} \approx \frac{\mathsf{N}_N(z)}{\mathsf{D}_M(z)} = \sum_{i=1}^{M}\frac{K_i}{z - z_i}, \tag{8}$$

[1]The probability distribution of the parameters $\mathbf{x}$ is possibly unknown, and hence disregarded here. Only the *possibility* to occur within their range of variation is considered.

where $\mathsf{N}_N(z)$ and $\mathsf{D}_M(z)$ are two polynomials, whereas z_i and K_i are the poles and the residues of the corresponding rational function, respectively. The coefficients of the polynomials $\mathsf{N}_N(z)$ and $\mathsf{D}_M(z)$ are available in closed form [15], and the poles and residues are readily computed from these.

By substituting (8) into (7), the time-domain response can be expressed as [14]

$$\begin{aligned} y(t) &\approx \frac{1}{j2\pi t}\int_{\sigma'-j\infty}^{\sigma'+j\infty} Y\left(\frac{z}{t}\right)\sum_{i=1}^{M}\frac{K_i}{z-z_i}dz \\ &= -\frac{1}{t}\sum_{i=1}^{\lceil M/2\rceil}\Re e\left\{\hat{K}_i Y\left(\frac{z_i}{t}\right)\right\}, \end{aligned} \tag{9}$$

where $\hat{K}_i = K_i$ for a real pole and $\hat{K}_i = 2K_i$ for a pair of complex conjugate poles.

It is worth noting that (9) features again a linear combination of a set of Laplace-domain responses but, as opposed to (6), it is not discretized. However, for each time instant t at which the response is evaluated, the response needs to be computed for a *different* set of $\lceil M/2\rceil$ complex frequencies. Furthermore, the accuracy is strongly related to the order M in the Padé approximation (8). As shown in the following application examples, a too low order M leads to poor accuracy in reproducing the dynamics of $y(t)$ at the end of the observation window. On the other hand, a large value of M may cause numerical issues. Therefore, it is in general difficult to properly choose the value of M.

C. NILT Based on IFFT and Convolution

This technique is presented to illustrate the advantage of pure spectral techniques with respect to convolution-based approaches. The underlying idea is to compute the time-domain response as the convolution between the impulse response of the system $h(t) = \mathscr{L}^{-1}\{H(s)\}(t)$, calculated via the NILT in (6), and the excitation $e(t)$:

$$y(t) = h(t) * e(t) = \int_0^{+\infty} h(t-\tau)e(\tau)d\tau. \tag{10}$$

The above integral is calculated as the following sum of discrete functions:

$$y[k\Delta_t] \approx \Delta_t \sum_{i=0}^{N} h[(k-i)\Delta_t]e[i\Delta_t] \quad \forall k,\, k-i \geq 0, \tag{11}$$

where Δ_t is the desired time step and the discrete-time impulse response is computed with (6). Equation (11) highlights the main difference between the pure spectral approaches and the integration-based (including ODE) ones for the self-validated analysis of linear time-invariant systems. Owing to the integral operator, each sample $y(t_k)$ is correlated to the system responses at previous time instants. Therefore, the TM remainder is likely to constantly grow and eventually blowup, as shown in the following. On the contrary, the solutions based on (6) and (9) turn out to be completely independent from the previous and future samples of $y(t)$.

IV. Application Examples

In this section, the TM framework is applied to the time-domain analysis of various linear systems with bounded uncertain parameters. To this end, the state-of-the-art TMsim toolbox [7], [8] is combined with the NILT implementations discussed in Section III by using available operations. Although the following application examples focus on the estimation of the output bounds, it is worth mentioning that the TMs provide in addition an accurate parametric representation of the outputs with respect to the uncertain input parameters.

A. Illustrative Example: Control Loop

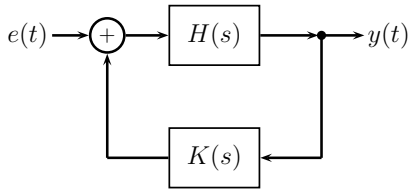

Fig. 1. Block diagram of the control loop system with a PID controller.

For the sake of illustration, the proposed method is first applied to simulate the time-domain response of the control loop in Fig. 1. The system consists of a closed loop with open-loop transfer function $G(s) = 1/(s^2 + 5s + 3)$ and a proportional integrative derivative (PID) controller feedback with transfer function $K(s) = c_1 + c_2/s + 0.1s$. The parameters c_1 and c_2 of the controller are independent uncertain variables in the intervals $c_1 = [8, 10]$ and $c_2 = [21, 29]$, respectively. These two variables are readily expressed as the following TMs:

$$T_{c_1}(x_1) = P_{c_1}(x_1) + I_{c_1} = 9 + 1 \cdot x_1 + [0, 0] \tag{12a}$$

$$T_{c_2}(x_2) = P_{c_2}(x_2) + I_{c_2} = 25 + 4 \cdot x_2 + [0, 0], \tag{12b}$$

where for computational convenience $\mathbf{x} = [x_1, x_2]$ is normalized within the domain $D = [-1, 1] \times [-1, 1]$. Starting from (12), the transfer function $K(s)$ of the controller is expressed as the multivariate TM

$$T_K(s; \mathbf{x}) = T_{c_1}(x_1) + \frac{T_{c_2}(x_2)}{s} + 0.1s. \tag{13}$$

Finally, the TM representation of the closed-loop transfer function $H(s; \mathbf{x})$ is obtained as

$$T_H(s; \mathbf{x}) = \frac{T_K(s; \mathbf{x})G(s)}{1 + T_K(s; \mathbf{x})} = P_H(s; \mathbf{x}) + I_H(s), \tag{14}$$

where P_H and I_H are calculated by means of the TMsim toolbox. This allows obtaining a conservative estimation of the upper and lower bounds of $H(s; \mathbf{x})$ for all the possible combinations of the uncertain parameters $[c_1, c_2] \in [8, 10] \times [21, 29]$.

A conservative estimation of the bounds of the time-domain response is obtained by calculating the corresponding TM via the NILT. As an example, a unit step excitation $e(t) = u(t - t_0)$, with $t_0 = 1$ s, is considered. Starting

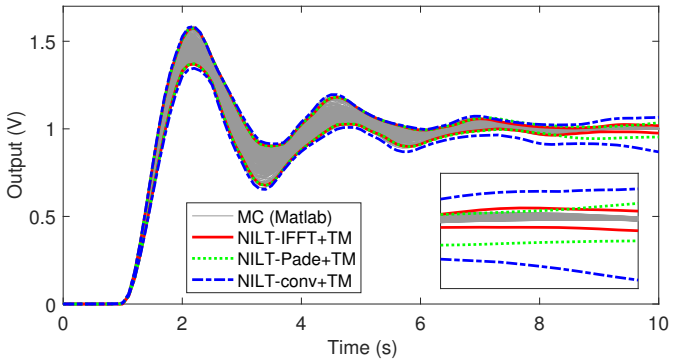

Fig. 2. Step response of the linear system of Fig. 1. Gray lines: MC samples; solid red, dotted green, and dashed blue lines: bounds from IFFT-, Padé approximation- and convolution-based TM analyses, respectively.

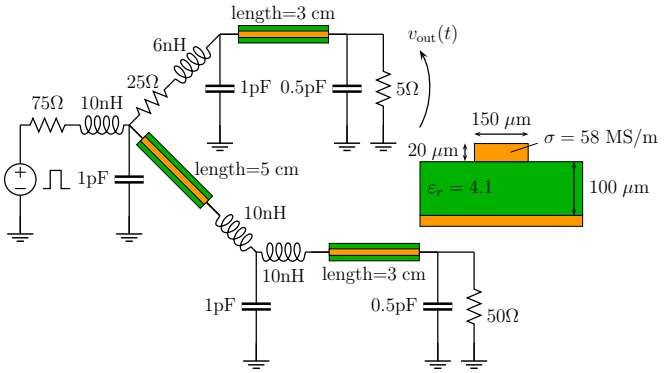

Fig. 3. Network consisting of microstrip lines and lumped elements. The cross-section of the lines is shown on the right.

from (14), the time-domain TM is computed as $T_y(t;\mathbf{x}) = \mathscr{L}^{-1}\{T_H(s;\mathbf{x})E(s)\}(t)$, with $E(s) = \mathscr{L}\{e(t)\} = 1/s\, e^{-st_0}$.

Fig. 2 shows the spread of the response resulting from the parameter uncertainty and obtained based on 10000 Monte Carlo (MC) samples. The bounds estimated from TM simulations with expansion order $n = 6$ and the different NILT implementations are also shown. The curves indicate that the IFFT-based NILT (solid red lines) provides a very tight enclose of the MC curves within the whole simulation window. On the contrary, the bounds obtained with both the Padé approximation- (dashed blue lines) and convolution-based (dotted green lines) approaches slightly diverge towards the end of the observation time. This is due to the high order in the approximation ($M = 12$) and to the integration in the two cases, respectively.

At this point, it is important to mention that the MC samples in Fig. 2 are computed via the IFFT-based NILT (6). For this specific example, however, the various NILT implementations do not have an appreciable effect on the deterministic calculation of the MC responses. Nonetheless, as discussed above, they do affect the TM remainder and hence the tightness of the estimated enclosure.

B. Lossy Transmission-Line Network

Next, the proposed technique is applied to the network of Fig. 3. The circuit consists of a combination of lossy microstrip transmission lines and lumped elements. The value of the inductors and the capacitors varies within 10% around the nominal value. The network is represented in the Laplace domain by means of the modified nodal analysis (MNA) formalism, leading to a linear system with 13 unknowns. The microstrip conductor resistance is modeled as $R_o + R_s\sqrt{s/\pi}$ to properly account for the skin effect [16]. The network is excited at the left side with a pulse of amplitude $E_0 = 1$ V, duration $T = 3$ ns and rise/fall times $\tau_r = \tau_f = 0.2$ ns.

Fig. 4 shows the resulting time-domain evolution of the far-end voltage v_{out} indicated in Fig. 3. The spread resulting from 10000 MC runs computed via the IFFT-based NILT (gray lines) is compared with the enclosures obtained by means of TM analyses of order $n = 5$. While the IFFT-based implementation (solid red lines) provides again a tight enclosure, the remainder of the convolution-based solution (dotted green lines) quickly blows up due to the integration. Furthermore, it is possible to appreciate how the Padé approximation computed with $M = 13$ (dashed blue lines) is unable to accurately capture the high dynamic of the waveform. Increasing the order M makes the analysis numerically instable and the response diverge. It should be noted that this inaccuracy appears also in the MC samples, while the convolution-based NILT still performs well for the deterministic MC calculations (results not shown here). These results confirm the better performance of the IFFT-based NILT in the TM analysis with respect to other approaches. Finally, for an independent validation, the bounds obtained from 10000 transient MC simulations in SPICE are shown by the dashed black lines. These results confirm the general accuracy of the IFFT-based NILT. However, there is no guarantee that the TM bounds are conservative with respect to the SPICE result, since the underlying solution algorithms differ.

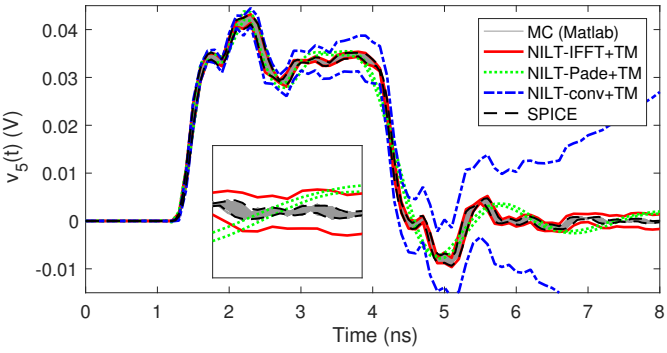

Fig. 4. Time-domain behavior of voltage v_{out} in the circuit of Fig. 3. Gray lines: MC samples; solid red, dotted green, and dashed blue lines: bounds from IFFT-, Padé approximation- and convolution-based TM analyses, respectively; dashed black lines: bounds from a transient MC analysis in SPICE.

As far as the computational times are concerned, the IFFT-, Padé approximation- and convolution-based TM simulations take 295 s, 507 s and 1153 s, respectively. For comparison, the MC analysis in SPICE requires 1540 s instead. This demonstrates that the IFFT-based approach provides, besides a superior accuracy, also higher computational efficiency. On

the other hand, the computational cost is competitive with a commercial circuit simulator, while providing in addition a parametric representation of the output.

C. Active Low-Pass Filter

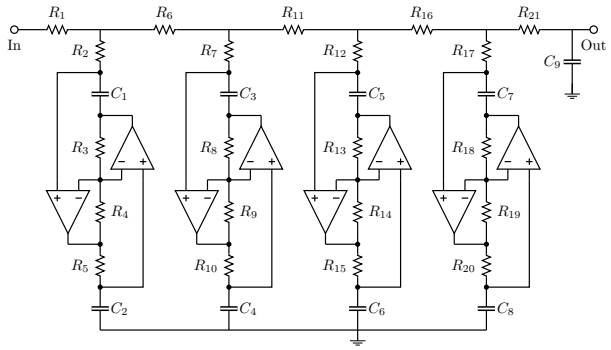

Fig. 5. Schematic of the low-pass filter reproduced from [17].

The last example considers the active low-pass filter in Fig. 6, consisting of a combination of ideal operational amplifiers and passive elements and having a bandwidth of approximately 3 kHz. The value of the capacitors C_2, C_8 and C_9 is assumed to vary within $[9.5, 10.5]$ nF. The network is described in the Laplace domain by means of the MNA, leading to a system of 17 equations. To stress the robustness of the proposed method, an out-of-band impulse, with amplitude 1 V and duration 0.167 ms, is considered as input.

Fig. 6 shows the time-domain behavior of the output voltage. The spread of 10000 MC simulations (gray lines) is compared with the enclosure obtained with a TM analysis ($n = 4$) in conjunction with the IFFT-based NILT (solid red lines), showing again excellent agreement. The MC bounds obtained with two transient SPICE simulations with different maximum time steps are provided by the dashed and solid black lines. These additional curves highlight the strong instability of the SPICE simulation as a function of the selected maximum time step, which is avoided by the Laplace-based analysis.

V. Conclusions

This paper addresses the self-validated time-domain analysis of linear systems affected by bounded uncertain parameters. The proposed technique effectively combines the framework of TMs with the NILT. Different NILT implementations are reviewed for this purpose. A NILT based on the IFFT provides the best performance in terms of both accuracy and computational efficiency. Three application examples are considered to support the discussion. The extension to circuits including nonlinear components is currently under investigation.

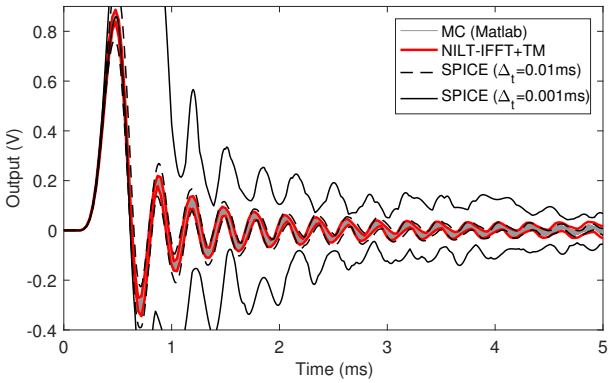

Fig. 6. Output voltage in the circuit of Fig. 6. Gray lines: MC samples; red lines: bounds from the TM analysis; dashed and solid black lines: bounds from SPICE MC simulations with different maximum time step.

References

[1] N. Femia and G. Spagnuolo, "Genetic optimization of interval arithmetic based worst case circuit tolerance analysis," *IEEE Trans. Circuits Syst. I, Fundam. Theory Appl.*, vol. 46, no. 12, pp. 1441–1456, Dec. 1999.

[2] N. Femia and G. Spagnuolo, "True worst-case circuit tolerance analysis using genetic algorithms and affine arithmetic," *IEEE Trans. Circuits Syst. I, Fundam. Theory Appl.*, vol. 47, no. 9, pp. 1285–1296, Sep. 2000.

[3] T. Ding, R. Trinchero, P. Manfredi, I. S. Stievano, and F. G. Canavero, "How affine arithmetic helps beat uncertainties in electrical systems," *IEEE Circuits Syst. Mag.*, vol. 15, no. 4, pp. 70–79, Nov. 2015.

[4] K. Makino and M. Berz, "Remainder differential algebras and their applications," in *Computational Differentiation: Techniques, Applications, and Tools*, SIAM, 1996.

[5] K. Makino and M. Berz, "Taylor models and other validated functional inclusion methods," *Int. J. Pure Appl. Math.*, vol. 4, no. 4, pp. 379–456, 2003.

[6] R. Trinchero, P. Manfredi, T. Ding, and I. S. Stievano, "Combined parametric and worst-case circuit analysis via Taylor models," *IEEE Trans. Circuits Syst. I, Fundam. Theory Appl.*, vol. 63, no. 7, pp. 1067–1078, Jul. 2016.

[7] R. Trinchero, P. Manfredi, and I. S. Stievano, "TMsim: an algorithmic tool for the parametric and worst-case simulation of systems with uncertainties," *Math. Problems Eng.*, vol. 2017, Article ID 6739857, 12 pages, 2017.

[8] [Online] https://www.tmsim.polito.it/

[9] M. Berz and K. Makino, "Verified integration of ODEs and flows using differential algebraic methods on high-order Taylor models," *Rel. Computing*, vol. 4, no. 4, pp. 361–369, 1998.

[10] M. Neher, K. R. Jackson, and N. S. Nedialkov, "On Taylor model based integration of ODEs," *SIAM J. Numerical Anal.*, vol. 45, no. 1, pp. 236–262, Jan. 2007.

[11] Y. Lin and M. A. Stadtherr, "Validated solutions of initial value problems for parametric ODEs," *Appl. Numerical Math.*, vol. 57, no. 10, pp. 1145–1162, Oct. 2007.

[12] L. M. Wedepohl, "'Power system transients: Errors incurred in the numerical inversion of the Laplace transform," in *Midwest Symposium on Circuits and Systems*, August, 1983.

[13] P. Moreno and A. Ramirez,"Implementation of the numerical Laplace transform: A review" *IEEE Trans. Power Delivery*, vol. 23, no. 4, pag. 2599–2609, Oct. 2008.

[14] Y. Tao, B. Nouri, M. S. Nakhla, M. A. Farhan and R. Achar, "Variability Analysis via Parameterized Model Order Reduction and Numerical Inversion of Laplace Transform," *IEEE Trans. Compon. Packag. Manuf. Techol.*, vol. 7, no. 5, pp. 678–686, May 2017.

[15] J. Vlach, K. Singhal, "Computer Methods for Circuit Analysis and Design", Boston, MA, USA: Kluwer, 2003.

[16] C. R. Paul, Analysis of Multiconductor Transmission Lines.NewYork,NY, USA: Wiley-Interscience, 2008.

[17] T.-A. Pham, E. Gad, M. S. Nakhla, and R. Achar, "Decoupled polynomial chaos and its applications to statistical analysis of high-speed interconnects," *IEEE Trans. Compon. Packag. Manuf. Techol.*, vol. 4, no. 10, pp. 1634–1647, Oct. 2014.